Clinical Immunology (2008) **128**, 155–163

available at www.sciencedirect.com

ScienceDirect

www.elsevier.com/locate/yclim

Mapping of binding epitopes of a human decay-accelerating factor monoclonal antibody capable of enhancing rituximab-mediated complement-dependent cytotoxicity

Bo Guo [a,1], Zheng-wei Ma [b,1], Hua Li [a], Gui-lian Xu [a], Ping Zheng [a], Bo Zhu [a], Yu-Zhang Wu [a], Qiang Zou [c,*]

[a] *Institute of Immunology, Third Military Medical University, District Shapingba, Chongqing 400038, PR China*
[b] *Institute of Hepatobiliary Surgery & Southwest Hospital, Third Military Medical University, District Shapingba, Chongqing 400038, PR China*
[c] *Department of Immunology, Chengdu Medical College, 601 Tianhui Road, Rongdu Aveneu, Chengdu 610083, PR China*

Received 21 November 2007; accepted with revision 17 March 2008
Available online 23 May 2008

KEYWORDS
Decay-accelerating factor;
Monoclonal antibody;
Complement-dependent cytotoxicity (CDC);
Tumor;
Immunotherapy

Abstract Complement-dependent cytotoxicity (CDC) is thought to be one of the most important mechanisms of action of therapeutic monoclonal antibodies (mAbs). The decay-accelerating factor (DAF) overexpressed in certain tumors limits the CDC effect of the therapeutic anticancer antibodies. The use of DAF blocking antibodies targeted specifically at cancer cells in combination with immunotherapeutic mAbs of cancer may improve the therapeutic effect in cancer patients. In this study, the lysis of Raji cells mediated by CDC was determined after blocking DAF function by anti-DAF polyclonal antibody and 3 mAbs (DG3, DG9, DA11) prepared in our laboratory, respectively, in the presence of the anti-CD20 chimeric mAb rituximab. The binding domains of the three anti-DAF mAbs were identified using yeast surface display technique, and the mimic epitopes of mAb DG3 were screened from a random phage-display nonapeptide library. The results showed that blocking DAF function by anti-DAF polyclonal antibody enhanced complement-mediated killing of Raji cells. Among the 3 mAbs against DAF, only DG3 was found to be able to remarkably enhance the CDC effect of the therapeutic mAb rituximab. DG3 bound to the third short consensus repeat (SCR) of DAF. Binding of DG3 to immobilized DAF was inhibited by mimic epitope peptides screened from the peptide library. Our results suggest that a higher level of DAF expressed by certain tumor cells is significant to abolish the CDC effect of therapeutic anticancer antibodies, and mAbs binding to SCR3 can enhance the complement-mediated killing of Raji cells. It is of significance to identify

Abbreviations: mAb, monoclonal antibody; CDC, complement-dependent cytotoxicity; mCRPs, membrane complement regulatory proteins; DAF, decay-accelerating factor; SCR, short consensus repeat; NHS, normal human serum.

* Corresponding author.
E-mail address: qiangzou99@gmail.com (Q. Zou).

[1] These authors contributed equally to the manuscript.

1521-6616/$ – see front matter
doi:10.1016/j.clim.2008.03.507

the DAF epitopes required in inhibiting CDC not only for better understanding of the relationship between the structure and function of DAF, but also for designing and developing anti-DAF mAbs capable of enhancing CDC.

Introduction

Over recent years, the therapy with monoclonal antibodies (mAbs) has become a promising approach to the treatment of cancer due to the ability of mAbs to recognize specific cancer cells [1]. For instance, the anti-CD20 chimeric mAb rituximab has been successfully used to treat B-cell non-Hodgkin lymphoma (B-NHL) [2,3]. Complement-dependent cytotoxicity (CDC) is thought to be one of the most important mechanisms of action of therapeutic mAbs.

It has been reported that the CDC effect of therapeutic anticancer antibodies is significantly limited because certain cancer cells can resist complement-mediated cell lysis due to a higher expression of membrane complement regulatory proteins (mCRPs). It is envisaged that the use of mCRP blocking antibodies targeted specifically at cancer cells in combination with immunotherapeutic mAbs of cancer will improve the therapeutic effect in cancer patients [4–6]. However, the binding epitopes of these antibodies remain unclear.

Decay-accelerating factor (DAF, CD55), a membrane-bound complement regulatory protein, protects the normal tissue from accidental injury by activated complements. The expression of DAF was found to be up-regulated in certain tumors than in the normal tissue [7,8]. It was suggested that the turnover of CD55 on the cancer cell surface is an important factor influencing the resistance of cancer cells to CDC. Therefore, to control complement resistance related to DAF, e.g., to down-regulate CD55 expression, is becoming a target for tumor therapy [10,11]. It is of significance to develop neutralizing mAbs specific to DAF and identify the binding epitopes of these DAF mAbs for enhancing CDC induced by immunotherapeutic mAbs as well [6].

In order to identify the binding epitopes of human DAF mAbs capable of improving the therapeutic efficacy of anticancer antibodies, we investigated the effects of 3 specific DAF mAbs and a specific DAF polyclonal antibody prepared in our laboratory [12] on CDC of Raji cells induced by the immunotherapeutic mAb rituximab. We found that, among the 3 monoclonal antibodies specific to DAF, i.e. DG3, DG9 and DA11, only DG3 enhanced the CDC effect of the therapeutic mAb rituximab. Furthermore, the SCRs binding to these mAbs were identified by yeast surface display technique, and the binding epitopes of DG3 were screened from a phage peptide library. The present study may help better understand the relationship between the structure and function of DAF and investigate the mechanisms by which mCRPs decrease the CDC effect in certain cancer cells. Moreover, this study may promote the design and development of anti-DAF mAbs capable of enhancing the CDC effect.

Materials and methods

Preparation of antibodies and F(ab')2

Rituximab (anti-human CD20) was obtained from Genentech, Inc. (San Francisco, CA). The IgG1 mAbs DG3, DG9 and DA11 specific to the human DAF were prepared as described previously [12]. Briefly, the human DAF was purified from human erythrocytes by trypsin digestion, butanol extraction, sequential chromatography on DE32 and immunoaffinity chromatography (Pharmacia). Approximately 420 μg of the purified DAF was obtained from 400 mL of human whole blood. The activity recovery of the purified DAF was 26% and the specific activity of the purified DAF was 4.5×10^5 units/mg. SDS-PAGE of the purified protein resulted in a single band and the purified protein had an apparent molecular weight of about 70×10^3. Western blotting showed that the DAF monoclonal antibody can bind to the purified protein specifically and also inhibit the assembly and accelerate the decay of the classical pathway C3 convertase. Balb/c mice were immunized by injection of the partly purified human DAF to stimulate the production of specific antibodies. The antibody-producing cells were isolated from the mouse spleen. Single antibody-producing cells were fused to the P2/0 myeloma cells to form hybridomas to produce mAbs. After 8–12 days of culture of the hybridomas, the culture supernatants were used to screen mAbs by indirect ELISA. Three mAbs were obtained and named DG3, DG9 and DA11, respectively. Ascites was collected from the mice. Indirect ELISA revealed the titers of specific antibodies in culture supernatants and ascites to be 10^{-3}–10^{-4} and 10^{-6}–10^{-7}, respectively. Antibody isotypes were identified according to the manufacturer's protocol (Boehringer Mannheim, Cat. No. 1493027). All of the three mAbs were found to be IgG1 kappa isotypes.

F(ab')2 Ab fragments of DG3, DG9 and DA11 were prepared from the above mentioned mAbs by digestion with resin immobilized-ficin and protein A gel chromatography according to the manufacturer's protocol (Immunopure Kit No. 44880; Pierce, Rockford, IL). The IgG fraction of the mouse anti-human DAF polyclonal antibody and nonimmune serum were purified by chromatography on a protein G-Sepharose column (Pharmacia). F(ab')2 fragments of the mouse anti-human DAF polyclonal antibodies were prepared by digestion with pepsin (Sigma Chemical, St Louis, MO) for 4 h at 37 °C at an enzyme ratio of 1/600 (w/w) and purified by fast protein liquid chromatography using a MonoQ column (Pharmacia). The purity of the fragments was verified by SDS-PAGE. FITC-conjugated goat anti-mouse IgG, FITC-conjugated goat anti-human IgG and peroxidase-conjugated goat anti-mouse IgG antibodies were purchased from Sigma (St Louis, MO, USA).

Cell line and sera

Raji cell line was obtained from American Type Culture Collection (ATCC, Manassas, VA) and maintained in log phase growth at 37 °C in 5% CO_2 in RPMI 1640 complete media supplemented with 10% fetal bovine serum and penicillin/streptomycin (Gibco BRL, Grand Island, NY). Cells grown to the late logarithmic phase of growth were used for cell-killing assay. Normal human serum (NHS) served as a source of complements. NHS was prepared from coagulated blood of

healthy volunteers and stored in aliquots at −70 °C before use.

Flow cytometry

Flow cytometry was used to analyze the expression of DAF and CD20 on Raji cells and yeast surface display of DAF fragments. To block the binding of nonspecific immunoglobulins to Fc-receptors of Raji cells, Raji cells were incubated for 15 min with heat-inactivated human serum (diluted 1:10 in 0.5% bovine serum albumin (BSA)/phosphate-buffered saline (PBS)). Raji cells were washed twice with 0.5% BSA/PBS and incubated with DAF specific mAb DG3 or rituximab for 30 min on ice.

DAF fragments displayed by yeasts were incubated for 30 min on ice with the DAF specific mAbs DG3, DG9 or DA11. All antibodies were used at a final concentration of 10 μg/mL. After incubation, the cells were washed twice before 30 min of incubation with FITC-conjugated goat anti-mouse IgG or FITC-conjugated goat anti-human IgG (diluted 1:100 in 0.5% BSA/PBS). For negative controls, the cells were incubated without the primary antibody. Immunofluorescence was analyzed using a BD FACScan flow cytometer (BD Immunocytometry Systems) with a standard filter set-up.

CDC assay

Raji cells were labeled with ^{51}chromium (^{51}Cr) by incubating them with 100 mCi of $Na_2\ ^{51}CrO_4$ (Amersham International, Buckinghamshire, UK) for 1.5 h in 500 μL RPMI–10% FCS at 37 °C. The cells were washed three times with RPMI, incubated (10^6 cells/mL) with 20 μg/mL rituximab in 500 μL RPMI–10% FCS at 37 °C for 30 min, and then with blocking antibodies for 30 min at 4 °C. The cells were washed twice again and diluted in an appropriate amount of medium to a cell concentration of 1×10^5 cells/mL.

For CDC assay, 100 μL of ^{51}Cr labeled target Raji cells (1×10^4 cells) was plated into each well of a U-bottom 96-well microplate. Normal human serum was added as a source of complements and the samples were incubated for 30 min at 37 °C (a total volume of 200 μL). After centrifugation for 5 min at 500 ×*g*, 100 μL of the supernatants were subjected to radioactivity measurement using a gamma counter. The cell lysis rate in percentage was calculated using the formula below:

$$\text{Cell lysis}(\%) = \left[\left(^{51}\text{Cr released from sample} - {}^{51}\text{Cr released spontaneously}\right) / \left(\text{maximum } {}^{51}\text{Cr released} - {}^{51}\text{Cr released spontaneously}\right)\right] \times 100\%$$

All experiments were performed at least three times. The spontaneous release of ^{51}Cr from sample cells was <15% of the maximum release of ^{51}Cr, as determined by using the complete sample cell lysates obtained by treating the sample cells with 1% Triton X-100.

Yeast surface display of DAF fragments

A series of overlapping DAF fragments, SCR12 (residues 35–161), SCR23 (97–223), SCR34 (162–284) and SCR1234 (35–284) were produced by PCR. The fragments were cloned into the pYD1 yeast display plasmids (Invitrogen, Carlsbad, CA, USA). Then, the pYD1 yeast display plasmids modified to contain the genes encoding the DAF fragments were transformed into the yeast strain EBY100 by the LiAc/SS-DNA/PEG procedure [13]. DAF proteins were expressed on the yeast cell surface by using a commercially available kit (pYD1 Yeast Display Vector Kit, Catalog no. V835-01, Invitrogen Corporation, Carlsbad, CA) according to the manufacturer's protocol. Briefly, the transformed colonies were grown at 30 °C in minimal media containing yeast nitrogen base, casein hydrolysate, dextrose and phosphate buffer (pH 7.4) on a shaking platform for approximately one day until an OD_{600} of 5–6 was reached. Yeast cells were then induced to display proteins by transferring them to minimal media containing galactose and incubating them on a shaking platform at 30 °C for 36 h. The cultures were then stored at 4 °C before flow cytometric analysis.

Screening of phage peptide libraries with mAb DG3

The DG3 binding epitopes were analyzed by phage-display technique. A peptide library composed of random nonamers displayed on filamentous phages as fused to the N terminus of the major coat protein pVIII (pVIII9aa) was used [14]. Three rounds of biopanning were carried out. The clones were selected by biopanning performed essentially as previously described [15]. Briefly, a Petri dish (Falcon no.1008, Becton Dickinson and Co., Oxnard, CA) was coated overnight at 4 °C with 3 μg streptavidin/mL (Boerhinger-Mannheim, Germany). The Petri dish was subsequently washed three times with a washing buffer [PBS containing 0.1% (vol/vol) Tween 20]. Excessive binding sites were blocked for 90 min at 37 °C using a solution of 20 mM Tris–HCl (pH 7.5) and 150 mM NaCl (TBS) containing 1% BSA. About 10^{11} virions of the phage library were incubated for 1 h at room temperature with 10 μg of affinity-purified anti-DAF DG3 antibodies in 1 mL HBSS containing 0.1% BSA (The DG3 mAb concentration was 1 μg/mL in the second and third rounds of selection). To capture the phage–antibody complexes, 0.5 μg/mL biotinylated goat anti-mouse IgG was incubated for 30 min with the antibody–phage complexes. The Petri dish was washed four times and the phage–antibody complexes were added and incubated for 90 min at 37 °C. After four washes with the washing buffer, the phages were eluted from the Petri dish using 100 mM glycine–HCl (pH 2.2) and the eluents were transferred into another Petri dish. The pH value was adjusted to 8.5 with 1 M Tris–HCl. The eluted phages were added to 1.5 mL of *Escherichia coli* XL1–blue that had been cultured overnight, incubated 1 h at 37 °C and spread on LB agar plates containing 50 μg ampicillin/mL. After incubation overnight, the colonies were scraped and resuspended in 100 mL LB broth containing 50 μg ampicillin/mL to reach an OD_{600} value of 0.05. The cultures were incubated at 37 °C till the OD_{600} reached a value of 0.2 and then superinfected with M13KO7 to obtain the phage supernatants, which were precipitated twice with 4% polyethylene glycol (PEG) 8000–0.5 M NaCl. The amplified enriched library was subjected to further cycles of selection. Randomly chosen individual phage clones (a total of 100 clones) derived from the third round of biopanning were isolated, amplified and analyzed by phage ELISA. Microplates were coated overnight at 4 °C with phage clones (10^{10}) in PBS in a humidified chamber. The microplates were blocked with 200 μL of PBS–0.05% Tween 20 containing 5% defatted milk for 3 h at room

temperature. After four washes with the washing buffer (PBS–0.05% Tween 20, PBST), DG3 mAb was added to each well and incubated for 60 min at 37 °C. The microplates were washed four times and incubated for another 60 min at 37 °C with 100 μL of the peroxidase-conjugated goat anti-mouse IgG antibodies (Sigma, St Louis, MO, USA), diluted at a ratio of 1/4000 and washed four times again. The peroxidase activity retained in the wells was assayed by addition of 100 μL of 4 mg/mL *ortho*-phenylene diamine solution, followed by incubation for 20 min in dark at room temperature. The reaction was stopped by adding 50 μL of 2 M H_2SO_4 per well and the absorbance in each well was measured at 490 nm in a microplate reader. Thirteen positive clones were identified and sequenced by Sangon Biological Engineering Technology & Service Co., Ltd (Shanghai, China). The amino acid sequence of the clones was deduced from their nucleic acid sequence.

Competitive ELISA

Microplates were coated overnight at 4 °C with 50 μL of 0.04 μg/mL DAF (soluble recombinant DAF was a kind gift from Dr. Goodfellow, University of Reading, UK) in PBS. Non-specific binding sites were blocked by addition of 200 μL of PBS–0.1% Tween 20 containing 5% defatted milk. For competitive ELISA of the phage, various concentrations of the phage clone were incubated for 1 h at room temperature with 1 μg of anti-DAF DG3 affinity-purified antibodies in 200 μL HBSS containing 0.1% BSA. The phage clone–antibody complexes were added into the microplates and incubated for 1 h. For competitive ELISA of the peptide, a synthetic peptide (TPAWLDPPT) corresponding to the 12/13 phage sequence and a DAF SCR3 homologous peptide (SVQWSDPPT) were prepared by GL Biochem Ltd (Shanghai, China). Various concentrations of the peptides were incubated for 60 min at room temperature with 1 μg of anti-DAF DG3 antibodies in 1 mL HBSS containing 0.1% BSA. The peptide–DG3 complexes were added into microplates and incubated for 1 h. The microplates were washed four times with the washing buffer, incubated for another 60 min at 37 °C with 100 μL of peroxidase-conjugated goat anti-mouse IgG antibodies (Sigma, St Louis, MO, USA), diluted at a ratio of 1/4000 and washed four times again. The peroxidase activity retained in the wells was assayed by addition of 100 μL of 4 mg/mL *ortho*-phenylene diamine solution for 20 min in dark at room temperature. In the control, DG3, instead of a mixture of DG3 and phage or a mixture of DG3 and the synthetic peptide was added to the microplates coated with DAF. The reaction was stopped by adding 50 μL of 2 M H_2SO_4 per well and the absorbance in each well was measured at 490 nm in a microplate reader. Each microplate included a positive and a negative control. Specific inhibition in percentage was calculated using the formula below:

$$\text{Inhibition}\,(\%) = [(\text{OD}_{490}\ \text{of control} - \text{OD}_{490}\ \text{of sample})/\text{OD}_{490}\ \text{of control}] \times 100\%$$

Statistical analysis

All data shown are representative of at least three independent experiments. Data are expressed as mean ± SD. ANOVA was performed using SPSS 11.0 software for windows 2000. A p value <0.05 was considered statistically significant.

Results

Expression of DAF and CD20 on Raji cells

Raji cell line, derived from a Burkitt's lymphoma, was used in the present study. The expression of DAF and CD20 on Raji cell surface was determined by flow cytometry after Raji cells were stained with respective antibodies. The results (Fig. 1) showed that DAF and CD20 were positively expressed on Raji cell surface. The unimodal fluorescence profiles for the two molecules were narrow, suggesting that each exhibited a cell population with uniformly molecular expression.

F(ab')2 fragments of anti-DAF mAb DG3 increased complement-mediated lysis of Raji cells in the presence of rituximab

CDC is thought to be one of the most important mechanisms of action of therapeutic mAbs. It has been shown that the expression of DAF inhibits the CDC effect of immunotherapeutic mAbs [16]. Therefore, we tested CDC-mediated Raji cell lysis by in vitro ^{51}Cr-release assay. As shown in Figure 2A, increasing concentrations of the human serum was added as a source of complements in the presence of rituximab. Raji cells showed a complete resistance to cell lysis at the serum concentration of 6.25%, and only insignificant cell lysis at the

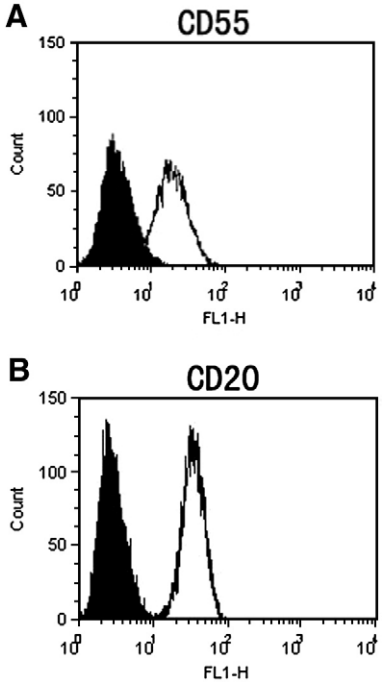

Figure 1 Expression of the complement regulatory protien CD55 and CD20 on the Raji lymphoma cell surface. Cells were stained with (A) DG3 (anti-CD55) and (B) rituximab (anti-CD20) monoclonal antibodies, respectively (open curves). Control staining was performed using irrelevant mouse or human immunoglobulin (IgG) as the primary antibody (hatched curves). Bound antibodies were detected with fluorescein isothiocyanate (FITC)-conjugated goat anti-mouse IgG (CD55) or goat anti-human IgG secondary antibody. After staining the cells were analyzed using flow cytometry.

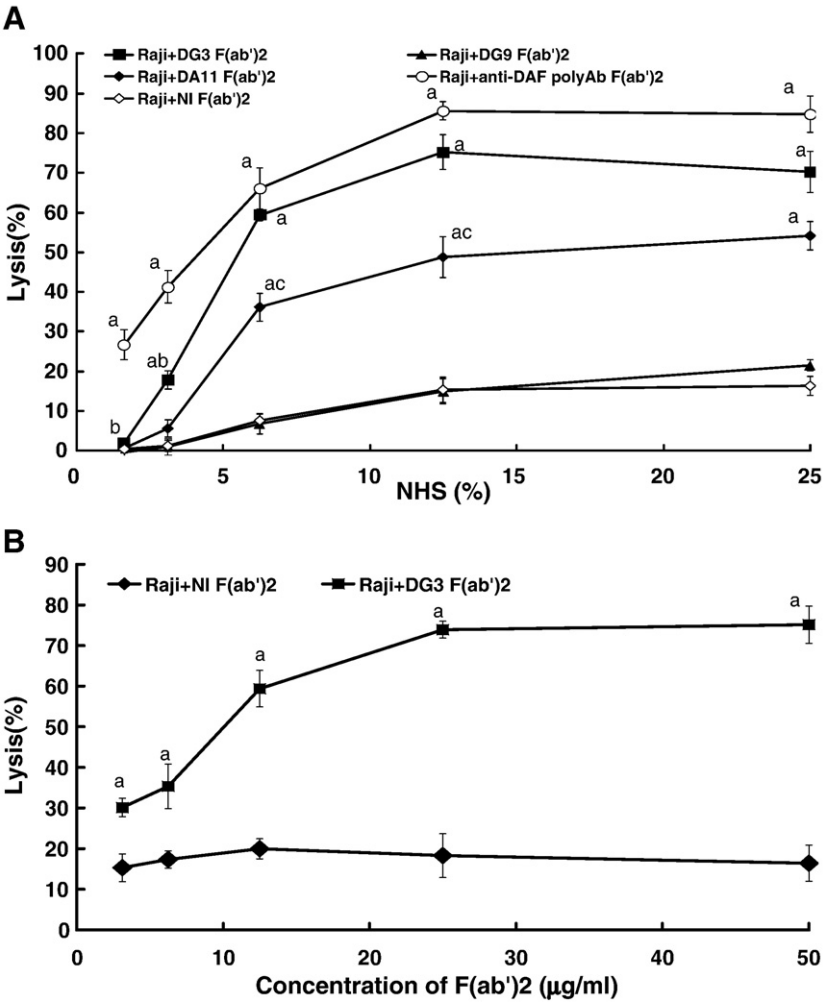

Figure 2 F(ab′)2 fragments of anti-CD55 resulted in enhanced Raji cell lysis by complement. (A) Raji were labeled with ^{51}Cr, sensitized with rituximab (20 μg/mL) for 30 min at 37 °C, and incubated with 20 μg/mL of anti-CD55 F(ab′)2 fragments respectively (■, DG3; ▲, DG9; ◆, DA11; ○, mouse anti-DAF polyclonal antibody; ◇, nonimmune mouse F(ab′)2) for 30 min at 4 °C. Then, cells were incubated with increasing dilutions of normal human serum for 1 h at 37 °C. The radioactivity was measured for each sample. Values represent mean ± SD from three similarly performed experiments. a: $p<0.05$, vs. Raji+NI F(ab′)2, b: $p<0.05$, vs. Raji+anti-DAF poly F(ab′)2; c: $p<0.05$, vs. Raji+DG3 F(ab′)2 at the same concentration of HHS. (B) The effect of anti-CD55 mAb DG3 F(ab′)2 on the complement-mediated cytolysis of the Raji cells in the presence of anti-CD20 mAb (rituximab; 20 μg/mL). NHS diluted at a ratio of 1:5 served as the complements source. 10^6 cells labeled with ^{51}Cr were incubated with the antibodies and NHS for 30 min at 37 °C. Lysis was measured as release of ^{51}Cr. Values represent mean ± SD from three similarly performed experiments. a: $p<0.05$, vs. Raji + NI F(ab′) at the same concentration of F(ab′)2.

serum concentration of 25% when the cells were incubated with F(ab′)2 antibodies derived from nonimmunized mice. In contrast, under the same conditions, when compared with F(ab′)2 antibodies derived from nonimmunized mice, adding mouse anti-DAF F(ab′)2 polyclonal antibody resulted in a significant increase in cell lysis ($p<0.05$), and Raji cells were readily killed even at a complement dilution of 1:64 in serum. These results suggested that the inhibition of DAF function in Raji cells by specific DAF antibody markedly increased the susceptibility of Raji cells to complement-mediated killing in the presence of rituximab.

To investigate the inhibitory sensitivity of the 3 specific DAF mAbs DG3, DG9 and DA11 prepared in our laboratory [12], the effects of these mAbs on the inhibition of DAF function in Raji cell lysis mediated by complements were compared with those of the mouse anti-DAF F(ab′)2 polyclonal antibody. As shown in Figure 2A, when compared with F(ab′)2 antibodies derived from nonimmunized mice, F(ab′)2 fragments of DG3 significantly reversed DAF-mediated inhibition of cell lysis in the presence of rituximab ($p<0.05$), and the effect was comparable to that of the mouse anti-DAF F(ab′)2 polyclonal antibody ($p>0.05$, DG3 vs. mouse anti-DAF F(ab′)2 polyclonal antibody). DA11 F(ab′)2 fragments showed markedly weaker inhibitory effects than DG3 F(ab′)2 fragments ($p<0.05$), though DA11 significantly reversed DAF-mediated inhibition of cell lysis in the presence of rituximab when compared with the F(ab′)2 fragments derived from nonimmunized mice ($p<0.05$). DG9 F (ab′)2 fragments showed little effects on DAF-mediated inhibition of cell lysis when compared with F(ab′)2 fragments derived from nonimmunized mice ($p>0.05$).

To explore whether the relative affinity of the mAbs fragments influences their effects, the relative affinity of the three mAbs fragments were determined. We found that the relative affinity of DG3 and DA11 fragments was similar, while the relative affinity of DG9 F(ab′)2 was about 10 times higher than that of DG3 and DA11 (data not shown). DG9 fragments had the highest relative affinity, but showed little effect on DAF-mediated inhibition of cell lysis, and DG3 had lower relative affinity, but significantly reversed DAF-mediated inhibition of cell lysis in the presence of rituximab. These results suggested that the relative affinity didn't play a role in the competitive mAb fragment-mediated effects and the lower relative affinity cannot explain the fact that DG9 fragments showed little effect on DAF-mediated inhibition of cell lysis.

To analyze the inhibitory sensitivity of DG3 to DAF in rituximab-mediated cell lysis, Raji cells were treated with increasing amounts of DG3 F(ab′)2 in the presence of rituximab (20 μg/mL) and NHS (at a final dilution of 1:5). As illustrated in Figure 2B, 73.9% of Raji cells were killed by 25 μg/mL DG3 F(ab′)2 during a 30-min incubation at 37 °C in the presence of rituximab plus NHS, and cell lysis was significantly lower when the concentration of DG3 F(ab′)2 was lower than 25 μg/mL ($p<0.05$). However, when the concentration of DG3 F(ab′)2 was higher than 25 μg/mL, no significant increase in cell lysis was observed. These results suggested that the optimal inhibitory concentration of DG3 F(ab′)2 was 25 μg/mL during a 30-min incubation at 37 °C in the presence of rituximab plus NHS.

DG3 bound to the domain of the third short consensus repeats of decay-accelerating factor

The DAF molecule from the N terminus consists of four SCRs, Ser/Thr-rich regions containing O-linked glycosylation sites and a membrane anchoring unit [17]. To probe the binding domains of the three anti-DAF mAbs, we produced fragments of the human DAF by yeast surface display, a useful method to identify stable folded protein domains from multidomain extracellular receptors, as well as to characterize antibody binding epitopes, without the need for soluble protein expression and purification [18]. Yeast-expressed wild-type DAF, and fragments of SCR12-DAF, SCR23-DAF and SCR34-DAF were tested for mAbs binding by indirect immunofluorescence using flow cytometry. The results showed that the mAb DG9 recognized both the yeast-displayed DAF fragment SCR12 and wild-type DAF (Fig. 3A), but did not recognize SCR23 or SCR34, demonstrating that the mAb DG9 epitope may be contained in the region of SCR1 or in the region between SCR1 and SCR2. The mAb DG3 bound to the yeast-displayed DAF fragments SCR23, SCR34 and wild-type DAF (Fig. 3B), but did not bind to SCR1, suggesting that the mAb DG3 epitope was contained in the region of SCR3, but not in the region of SCR1, SCR2 or SCR4. DA11 mAb recognized both the yeast-displayed DAF fragment SCR34 and the wild-type DAF (Fig. 3C), but not SCR12 or SCR23, indicating that the DA11 mAb epitope may be contained in the region of SCR4 or in the region between SCR3 and SCR4, but not in SCR1 or SCR2.

Mapping of DG3 mAb epitopes on DAF

To more precisely clarify the DG3 binding epitopes of the DAF SCR3 domain, amino acid sequences were selected from a random nonapeptide phage-display library by their affinity for the monoclonal antibody DG3 binding site.

A total of 100 clones were randomly chosen after the third round of screening and were subjected to ELISA. Thirteen clones were found to react strongly with DG3. All these phage clones were sequenced. These 13 clones comprised only two different

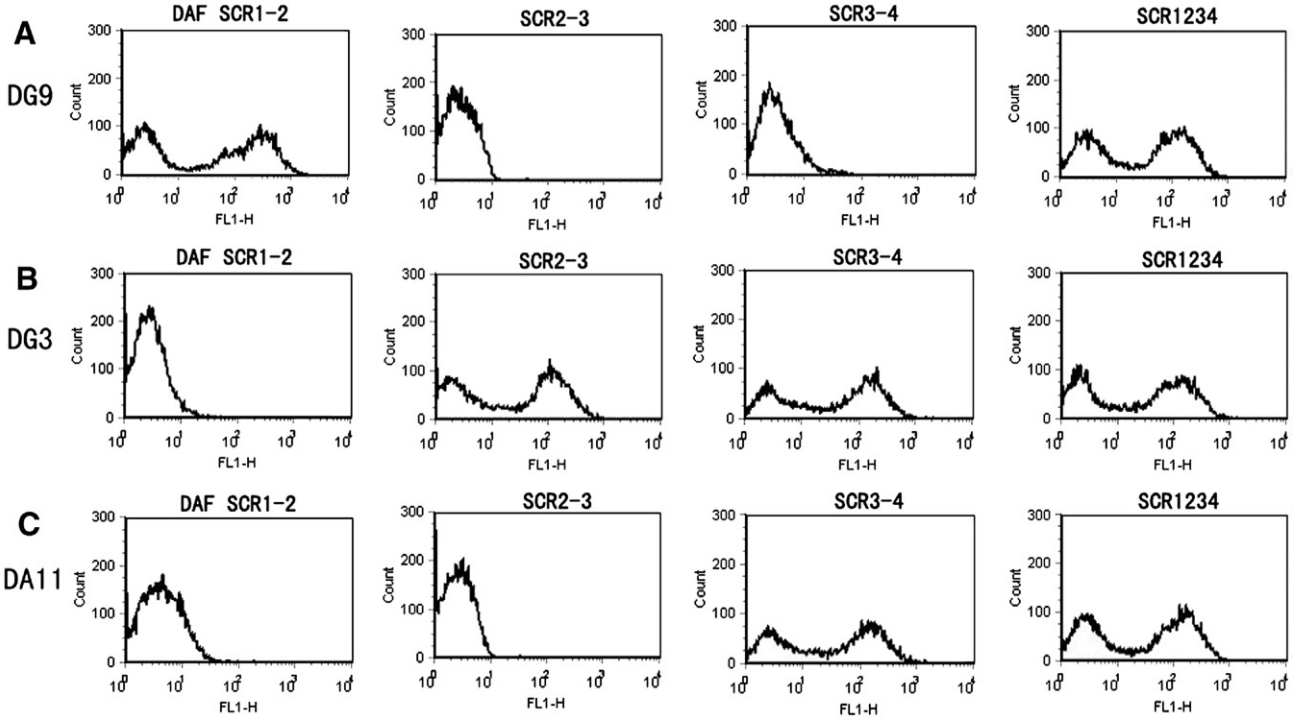

Figure 3 Anti-DAF mAbs domain mapping of yeast-displayed DAF fragments. Representative flow cytometry histograms depicting the mean fluorescence signal of DAF mAbs labeling of yeast-displayed DAF fragments. Data is representative of three experiments.

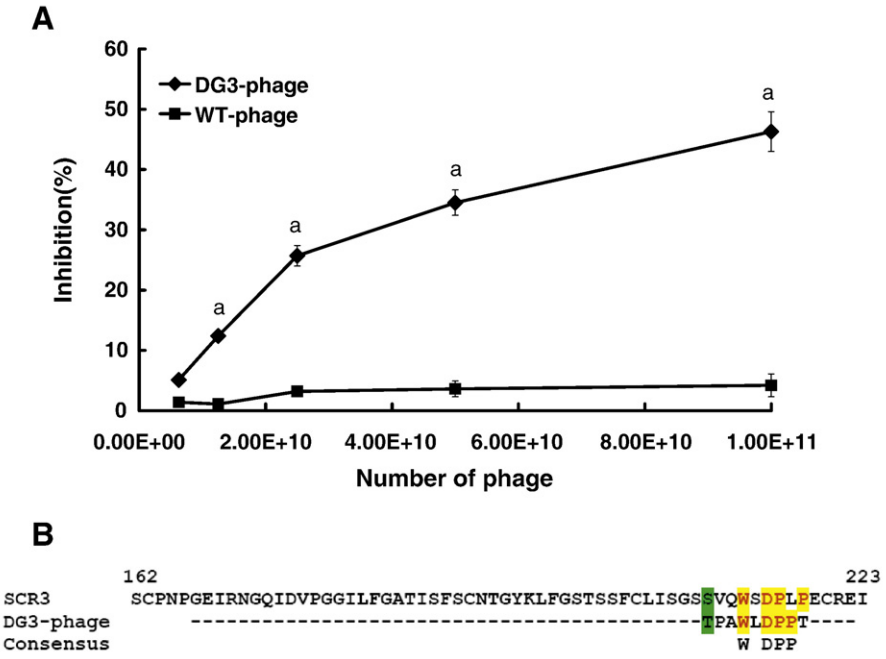

Figure 4 Inhibited binding of DAF to DG3 by DG3-phage (A) and mapping of DG3 epitope (B). DG3-phage represents 12/13 phage sequences eluted from three rounds of panning with DG3. (A). DAF was coated on each well of a microplate. DG3 was incubated with the immobilized DAF in the presence of DG3-phage or wild-type phage at the indicated concentrations, and the goat–anti-mouse IgG horseradish peroxidase was used as described in Materials and methods. The data are presented as mean ± SD from triplicate wells. a: $p<0.05$, vs. Raji + NI F(ab′)2 at the same number of phage. (B). Amino acid sequence alignment of DG3-phage and the domain SCR3 of DAF molecule.

sequences. One sample was an independent clone (PTAQRWRFR, frequency 1/13, phage 1), and the other 12 shared the same sequence (TPAWLDPPT, frequency 12/13, phage 2). Two isolated sequences did not show obvious homology.

Then, the specificity of the two different peptides to immobilized DAF was confirmed by competitive ELISA. The results showed that phage 2, but not phage 1, inhibited the binding of DG3 to immobilized DAF in a concentration-dependent manner, demonstrating the specificity of phage 2 to DG3 (Fig. 4A).

The amino acid sequence similarity between the selected clones and DAF was investigated. As shown in Figure 4B, although no absolute consensus sequences were observed between phage 2 and the SCR3 of DAF, phage 2 showed sequence similarity with amino acids 210–218 of DAF SCR3, suggesting that DG3 recognized a nonlinear constrained epitope where, at least in part, SCR-3 contributed to this binding. Sequence homology between phage 2 and the DAF molecule was 44.4%(4/9), suggesting that the peptide

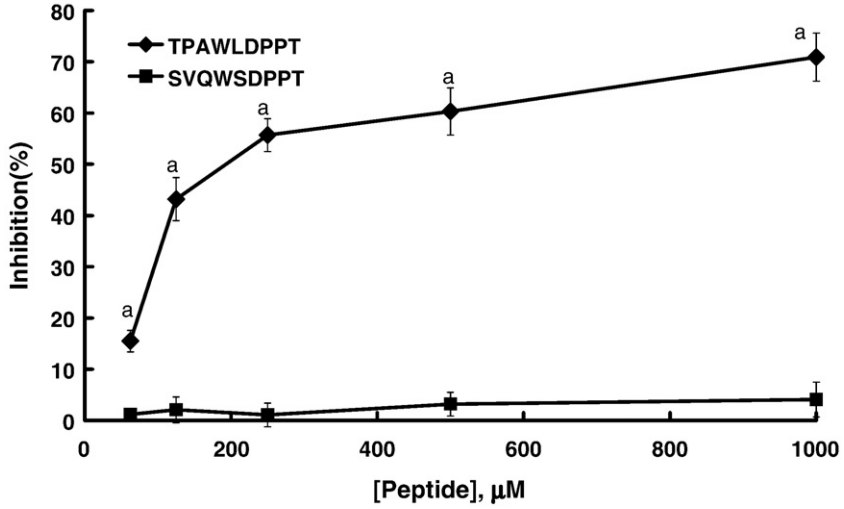

Figure 5 Binding of DAF to immobilized DG3 was inhibited by adding peptide TPAWLDPPT. DAF was coated on each well of a microplate. DG3 was incubated with the immobilized DAF in the presence of synthetic TPAWLDPPT peptide or DAF SCR3 homologous peptide (SVQWSDPPT) at the indicated concentrations, and the goat–anti-mouse IgG horseradish peroxidase was used as described in Materials and methods. The data are presented as mean ± SD from triplicate wells. a: $p<0.05$, vs. SVQWSDPPT at the same concentration of peptide.

TPAWLDPPT may correspond to a site of interaction between DG3 and the DAF molecule. To determine whether the peptide TPAWLDPPT mimics the structure of the DG3-binding epitope of DAF, competitive binding of DG3 and the peptide TPAWLDPPT with immobilized DAF was investigated by ELISA. As shown in Figure 5, the binding of DG3 to DAF was inhibited by adding the peptide TPAWLDPPT in a concentration-dependent manner, while the control peptide (DAF SCR3 homologous peptide, SVQWSDPPT) had no effect on the binding of DG3 to DAF. These data support that the peptide TPAWLDPPT mimics the DG3-binding epitope of DAF, and that DG3 recognizes a nonlinear constrained epitope.

Discussion

CDC is thought to be one of the most important mechanisms of action of therapeutic mAbs. In view of the fact that only half of patients with non-Hodgkin lymphoma respond to rituximab therapy [2,19,20], attempts to increase the efficacy of this treatment require an understanding of the mechanism by which tumor cells escape CDC.

Several studies suggested that the up-regulated expression of complement regulatory proteins may explain why lymphomas in some patients are refractory to the treatment with rituximab [21–23]. Using Raji cells as a model, we demonstrated that blocking DAF by both DAF mAb and mouse anti-DAF polyclonal antibody increased complement-mediated cell lysis in the presence of rituximab. The enhanced killing of Raji cells by mouse anti-DAF polyclonal antibody in the presence of rituximab is noteworthy (Fig. 2). Our results imply that DAF plays an important role in the inhibition of rituximab-mediated killing of Raji cells, and that up-regulation of DAF expression on cancer cells may block the action of immunotherapeutic modalities involved CDC.

To further clarify the roles of DAF in CDC, the three anti-DAF mAbs, DG3, DG9 and DA11, were developed in our laboratory and used to block the function of DAF in rituximab-mediated cell lysis. We found that DG3 F(ab′)2 abolished the inhibitory effect of DAF on complement-mediated cell lysis, and that DA11 had a weaker effect than DG3, and DG9 had no effect on CDC.

To understand the different roles of DG3, DG9 and DA11 in rituximab-mediated CDC, the binding domains of these mAbs were investigated. Using yeast surface display technique, we identified the DG3 epitope in the region of SCR3, the DG9 epitope in the region of SCR1 or in the region between SCR1 and SCR2, and the DA11 epitope in the region of SCR4 or in the region between SCR3 and SCR4 (Fig. 5). Several mAbs against human DAF have been reported [24–27]. However, only those antibodies binding to SCR3 block DAF function, such as 1C6, 1H4 and BRIC 216 mAbs. Our results provided additional evidence supporting the key functional role of SCR3. Previous studies [24,28] found that the regulatory function of the classical pathway C3 convertase depends on SCR2 and SCR3 of DAF. In this study, in the presence of rituximab, Raji cells were lyzed by human complements mainly via the classical pathway of complement activation. Remarkably, our results indicated that DA11 enhanced CDC in the presence of rituximab as well, although the effect of DA11 was weaker than that of DG3. This suggests that SCR4 is also required for the complement regulatory function of DAF in the classical complement activation pathway. The results also showed that both DG3 and DA11 blocked the function of DAF, which may explain the finding that the mouse anti-DAF polyclonal antibody was stronger than single mAbs in enhancing rituximab-mediated CDC (Fig. 2).

The mapping of mAb epitopes will be useful for future research, including the design of specific antibodies capable of blocking the function of DAF in CDC. To more precisely locate the binding sites of DG3 in DAF, we screened phages from a 9-mer phage-display library using DG3. We identified and characterized DG3 that recognized the mimotope (TPAWLDPPT), and this peptide had sequence similarity with the amino acids 210–218 (SVQWSDPPT) of DAF SCR3. However, the binding of DG3 to DAF was inhibited by adding the peptide TPAWLDPPT in a concentration-dependent manner, other than by the DAF SCR3 homologous peptide SVQWSDPPT. This is not surprising because phages or peptides can also recognize complex, discontinuous epitopes [29,30]. These results suggest the amino acids TPA contribute to the binding of DG3 to DAF and be the main recognition residues. Our attempts to define conformational epitopes corresponding to the DG3 binding site using a disulfide-constrained 9-mer library resulted in no specific phage amplification or selection (data not shown). We still do not know whether the peptide TPAWLDPPT inhibits complement activation, although ELISA showed that this functional peptide mimicked the structure of the DG3-binding epitope of DAF and blocked the binding of DG3 to DAF.

In conclusion, we demonstrated here that the use of specific anti-DAF antibodies in combination with rituximab enhanced complement-mediated Raji cell lysis. This suggests that the use of mAbs specific to DAF may be an advisable way to enhance the therapeutic efficacy of antitumor mAbs in certain tumor patients. This study indicated that DG3 bound to SCR3 and enhanced the complement-mediated Raji cell lysis, which may help utilize the therapeutic potential of rituximab. The yeast clones expressing different domains of DAF, together with three domain-specific mAbs, will be valuable resources for further investigating the important complement regulatory protein DAF. Moreover, the present study identified a mimetic peptide with potential to disrupt this DG3–DAF interaction. Such insights may promote the design and development of anti-DAF mAbs capable of enhancing CDC.

Acknowledgments

We thank Dr. Goodfellow for generously providing soluble recombinant DAF and Prof. P. Monaci for kindly providing the peptide library composed of random nonamers displayed on filamentous phages as fused to the N terminus of the major coat protein pVIII (pVIII9aa). This work was supported by grants NSFC 30471591 (to B. Guo), NSFC 30400436 (to Z.W. Ma) and NSFC 30772771 (to Q. Zou) from the National Natural Science Foundation of China.

References

[1] M. Harris, Monoclonal antibodies as therapeutic agents for cancer, Lancet Oncol. 5 (2004) 292–302.
[2] A.J. Grillo-Lopez, C.A. White, C. Varns, D. Shen, A. Wei, A. Mcclure, B.K. Dallaire, Overview of the clinical development of rituximab: first monoclonal antibody approved for the treatment of lymphoma, Semin. Oncol. 26 (1999) 66–73.

[3] P. Mclaughlin, C.A. White, A.J. Grillo-Lopez, D.G. Maloney, Clinical status and optimal use of rituximab for B-cell lymphomas, Oncology (Huntingt) 12 (1998) 1763–1769.
[4] Z. Fishelson, N. Donin, S. Zell, S. Schultz, M. Kirschfink, Obstacles to cancer immunotherapy: expression of membrane complement regulatory proteins (mCRPs) in tumors, Mol. Immunol 40 (2003) 109–123.
[5] K.A. Gelderman, V.T. Blok, G.J. Fleuren, A. Gorter, The inhibitory effect of CD46, CD55, and CD59 on complement activation after immunotherapeutic treatment of cervical carcinoma cells with monoclonal antibodies or bispecific monoclonal antibodies, Lab. Invest. 82 (2002) 483–493.
[6] P. Macor, C. Tripodo, S. Zorzet, E. Piovan, F. Bossi, R. Marzari, A. Amadori, F. Tedesco, In vivo targeting of human neutralizing antibodies against CD55 and CD59 to lymphoma cells increases the antitumor activity of rituximab, Cancer Res. 67 (2007) 10556–10563.
[7] L.G. Durrant, M.A. Chapman, D.J. Buckley, I. Spendlove, R.A. Robins, N.C. Armitage, Enhanced expression of the complement regulatory protein CD55 predicts a poor prognosis in colorectal cancer patients, Cancer Immunol. Immunother. 52 (2003) 638–642.
[8] S. Hiraoka, M. Mizuno, J. Nasu, H. Okazaki, C. Makidono, H. Okada, R. Terada, K. Yamamoto, T. Fujita, Y. Shiratori, Enhanced expression of decay-accelerating factor, a complement-regulatory protein, in the specialized intestinal metaplasia of Barrett's esophagus, J. Lab. Clin. Med. 143 (2004) 201–206.
[9] B.S. Ellison, M.K. Zanin, R.J. Boackle, Complement susceptibility in glutamine deprived breast cancer cells, Cell Div. 2 (2007) 20.
[10] Y. Terui, T. Sakurai, Y. Mishima, Y. Mishima, N. Sugimura, C. Sasaoka, K. Kojima, M. Yokoyama, N. Mizunuma, S. Takahashi, Y. Ito, K. Hatake, Blockade of bulky lymphoma-associated CD55 expression by RNA interference overcomes resistance to complement-dependent cytotoxicity with rituximab, Cancer Sci. 97 (2006) 72–79.
[11] S. Zell, N. Geis, R. Rutz, S. Schultz, T. Giese, M. Kirschfink, Down-regulation of CD55 and CD46 expression by anti-sense phosphorothioate oligonucleotides (S-ODNs) sensitizes tumour cells to complement attack, Clin. Exp. Immunol. 150 (2007) 576–584.
[12] Q. Zou, P.R. Xie, P. Zheng, Preparation and identification of mAbs against human decay-accelerating factor, Immunol. J. 15 (1999) 122–124.
[13] R.D. Gietz, R.H. Schiestl, A.R. Willems, R.A. Woods, Studies on the transformation of intact yeast cells by the LiAc/SS-DNA/PEG procedure, Yeast 11 (1995) 355–360.
[14] C. Prezzi, M. Nuzzo, A. Meola, P. Delmastro, G. Galfre, R. Cortese, A. Nicosia, P. Monaci, Selection of antigenic and immunogenic mimics of hepatitis C virus using sera from patients, J. Immunol. 156 (1996) 4504–4513.
[15] F. Felici, L. Castagnoli, A. Musacchio, R. Jappelli, G. Cesareni, Selection of antibody ligands from a large library of oligopeptides expressed on a multivalent exposition vector, J. Mol. Biol. 222 (1991) 301–310.
[16] J. Golay, L. Zaffaroni, T. Vaccari, M. Lazzari, G.M. Borleri, S. Bernasconi, F. Tedesco, A. Rambaldi, M. Introna, Biologic response of B lymphoma cells to anti-CD20 monoclonal antibody rituximab in vitro: CD55 and CD59 regulate complement-mediated cell lysis, Blood 95 (2000) 3900–3908.
[17] D.M. Lublin, J.P. Atkinson, Decay-accelerating factor: biochemistry, molecular biology, and function, Annu. Rev. Immunol. 7 (1989) 35–58.
[18] J.R. Cochran, Y.S. Kim, M.J. Olsen, R. Bhandari, K.D. Wittrup, Domain-level antibody epitope mapping through yeast surface display of epidermal growth factor receptor fragments, J. Immunol. Methods 287 (2004) 147–158.
[19] P. Colombat, G. Salles, N. Brousse, P. Eftekhari, P. Soubeyran, V. Delwail, E. Deconinck, C. Haioun, C. Foussard, C. Sebban, A. Stamatoullas, N. Milpied, F. Boue, B. Taillan, P. Lederlin, A. Najman, C. Thieblemont, F. Montestruc, A. Mathieu-Boue, A. Benzohra, P. Solal-Celigny, Rituximab (anti-CD20 monoclonal antibody) as single first-line therapy for patients with follicular lymphoma with a low tumor burden: clinical and molecular evaluation, Blood 97 (2001) 101–106.
[20] P. Mclaughlin, A.J. Grillo-Lopez, B.K. Link, R. Levy, M.S. Czuczman, M.E. Williams, M.R. Heyman, I. Bence-Bruckler, C.A. White, F. Cabanillas, V. Jain, A.D. Ho, J. Lister, K. Wey, D. Shen, B.K. Dallaire, Rituximab chimeric anti-CD20 monoclonal antibody therapy for relapsed indolent lymphoma: half of patients respond to a four-dose treatment program, J. Clin. Oncol. 16 (1998) 2825–2833.
[21] B. Bellosillo, N. Villamor, A. Lopez-Guillermo, S. Marce, J. Esteve, E. Campo, D. Colomer, E. Montserrat, Complement-mediated cell death induced by rituximab in B-cell lymphoproliferative disorders is mediated in vitro by a caspase-independent mechanism involving the generation of reactive oxygen species, Blood 98 (2001) 2771–2777.
[22] J. Golay, M. Lazzari, V. Facchinetti, S. Bernasconi, G. Borleri, T. Barbui, A. Rambaldi, M. Introna, CD20 levels determine the in vitro susceptibility to rituximab and complement of B-cell chronic lymphocytic leukemia: further regulation by CD55 and CD59, Blood 98 (2001) 3383–3389.
[23] K. Jurianz, S. Ziegler, H. Garcia-Schuler, S. Kraus, O. Bohana-Kashtan, Z. Fishelson, M. Kirschfink, Complement resistance of tumor cells: basal and induced mechanisms, Mol. Immunol. 36 (1999) 929–939.
[24] K.E. Coyne, S.E. Hall, S. Thompson, M.A. Arce, T. Kinoshita, T. Fujita, D.J. Anstee, W. Rosse, D.M. Lublin, Mapping of epitopes, glycosylation sites, and complement regulatory domains in human decay accelerating factor, J. Immunol. 149 (1992) 2906–2913.
[25] T. Hara, M. Matsumoto, Y. Fukumori, S. Miyagawa, M. Hatanaka, T. Kinoshita, T. Seya, H. Akedo, A monoclonal antibody against human decay-accelerating factor (DAF, CD55), D17, which lacks reactivity with semen-DAF, Immunol. Lett. 37 (1993) 145–152.
[26] M.E. Medof, E.I. Walter, W.L. Roberts, R. Haas, T.L. Rosenberry, Decay accelerating factor of complement is anchored to cells by a C-terminal glycolipid, Biochemistry 25 (1986) 6740–6747.
[27] W.D. Ratnoff, J.J. Knez, G.M. Prince, H. Okada, P.J. Lachmann, M.E. Medof, Structural properties of the glycoplasmanylinositol anchor phospholipid of the complement membrane attack complex inhibitor CD59, Clin. Exp. Immunol. 87 (1992) 415–421.
[28] W.G. Brodbeck, D. Liu, J. Sperry, C. Mold, M.E. Medof, Localization of classical and alternative pathway regulatory activity within the decay-accelerating factor, J. Immunol. 156 (1996) 2528–2533.
[29] G. Gevorkian, I. Petrushina, K. Manoutcharian, A. Ghochikyan, G. Acero, V. Vasilevko, D.H. Cribbs, M.G. Agadjanyan, Mimotopes of conformational epitopes in fibrillar beta-amyloid, J. Neuroimmunol. 156 (2004) 10–20.
[30] S.C. Wu, C.W. Lin, Neutralizing peptide ligands selected from phage-displayed libraries mimic the conformational epitope on domain III of the Japanese encephalitis virus envelope protein, Virus Res. 76 (2001) 59–69.